

Decomposition of a Double Salt Ionic Liquid Monopropellant on Heated Metallic Surfaces

Steven P. Berg¹ and Joshua L. Rovey²

Missouri University of Science and Technology, Rolla, Missouri, 65409

A monopropellant consisting of 59% hydroxylammonium nitrate and 41% 1-ethyl-3-methylimidazolium ethyl sulfate by mass is tested for decomposition on heated platinum, rhenium, and titanium surfaces. It was found that the propellant decomposes at 165 °C on titanium, which is the decomposition temperature of HAN. The onset temperature for decomposition on platinum was 85 °C and on rhenium it was 125 °C. This suggests that platinum and rhenium act as catalysts for the decomposition of the monopropellant. From the experimental data, Arrhenius-type reaction rate parameters were calculated. The activation energy for platinum was 3 times less than that of titanium suggesting it could be a prime choice for catalyst material in further thruster development.

Nomenclature

A	=	activity coefficient, [mL/mol-sec]
$C_{p,i}$	=	specific heat of species i , [J/kg-K]
E	=	activation energy, [J]
k'	=	reaction rate coefficient, [1/sec]
k_B	=	Boltzmann constant, [m ² -kg/sec ² -K]
N_i	=	number of moles of species i , [mol]
\dot{Q}	=	heat transfer rate, [W]
\dot{Q}''	=	heat flux, [W/mm ²]
\dot{Q}_E	=	heat transfer rate due to electrical heating, [W]
r_A	=	reaction rate, [mol/m-sec]
T	=	temperature, [K]
\dot{T}_{blank}	=	heating rate on blank surface, [K/s]
\dot{T}_E	=	electrical heating rate, [K/s]
\dot{T}_s	=	self heating rate, [K/s]
T_m	=	melting temperature, [K]
t	=	time, [sec]
V	=	volume, [m ³]
ΔH_{Rx}	=	heat of reaction, [J/mol]
ρ	=	resistivity, [Ω -m]
κ	=	thermal conductivity, [W/m-K]

I. Introduction

MULTI-mode spacecraft propulsion is the use of two or more propulsive devices on a spacecraft, specifically making use of a high-thrust, usually chemical, mode and a high-specific impulse, usually electric mode. This can be beneficial in two primary ways. One way a multi-mode propulsion system can be beneficial is by designing a mission such that the high-thrust and high-specific impulse maneuvers are conducted in such a way that it provides a

¹Postdoctoral Fellow, Aerospace Plasma Laboratory, Mechanical and Aerospace Engineering, 160 Toomey Hall, 400 W. 13th Street, Student Member AIAA.

²Associate Professor of Aerospace Engineering, Mechanical and Aerospace Engineering, 292D Toomey Hall, 400 W. 13th Street, Associate Fellow AIAA.

more efficient trajectory over a single chemical or single electric maneuver.¹⁻⁴ The second is to increase the mission flexibility of a single spacecraft architecture in that both high-thrust and high-specific impulse maneuvers are available to mission designers at will, perhaps even allowing for drastic changes in the mission plan while on-orbit or with a relatively short turnaround from concept to launch.⁵⁻⁷ For the second method, it is extremely beneficial to utilize a shared propellant for both modes as this provides the highest flexibility in terms of mission design choices. Two propellants have been developed which may function and theoretically perform well in both a chemical monopropellant and electric electrospray mode.⁸ These propellants, based on mixtures of ionic liquids [Emim][EtSO₄] and [Bmim][NO₃] with ionic liquid oxidizer hydroxylammonium nitrate (HAN), have been previously synthesized and assessed for thermal and catalytic decomposition in a microreactor.⁹ This paper presents results of further experiments to characterize the decomposition of the [Emim][EtSO₄]-HAN monopropellant, specifically on catalytic surfaces relevant to application in a microtube thruster¹⁰⁻¹² or similar geometry such as channels in a monolith catalyst. The electrospray capabilities of the propellants have been investigated previously.¹³

Hydrazine has been the monopropellant of choice for spacecraft and gas generators because it is storable, easily decomposed to give good performance properties, and has extensive flight heritage.¹⁴ However, hydrazine is also highly toxic and recent efforts have been aimed at replacing hydrazine with a high-performance, non-toxic 'green' monopropellant. Many of these efforts have focused on energetic ionic liquids, which are essentially molten salts with an energetic functional group and thus capable of rapid decomposition into gaseous products under proper stimulus. The energetic salts hydroxylammonium nitrate (HAN), ammonium dinitramide (ADN), and hydrazinium nitroformate (HNF) have received attention for this purpose.¹⁴⁻¹⁷ All of these salts have melting points above room temperature, and it is therefore necessary to use them in an aqueous solution to create a storable liquid propellant. Typically, these oxidizer rich ionic liquids are also mixed with a compatible fuel component to provide improved performance. The main limitation to the development of thrusters for these monopropellants has been excessive combustion temperatures, but recent efforts in materials and thermal management have mitigated some of these issues and flight tests have been conducted or are scheduled.¹⁷⁻¹⁹ These propellants, while performing well for chemical propulsion, fundamentally will not perform well in an electrospray thruster; therefore, for a proposed multi-mode monopropellant/electrospray system, novel system-specific propellants will be needed and the first generation has been synthesized.^{8,9}

Recent efforts have placed a greater emphasis on smaller spacecraft, specifically microsattellites (10-100 kg) and nanosatellites (1-10 kg), including the subset of cubesats. Many different types of thrusters have been proposed to meet the stringent mass and volume requirements placed on spacecraft of this type. Electrospray, in particular, may be well suited for micropropulsion, and has been selected for these types of applications.^{20,21} Many types of thrusters have been proposed for chemical propulsion for small spacecraft. One type is the chemical microtube.¹⁰⁻¹² This type of thruster is simply a heated tube of diameter ~1 mm or less that may or may not consist of a catalytic surface material. Additionally, from a multi-mode system standpoint, there is no fundamental reason why this geometry could not be shared with the electrospray mode as capillary type emitters can be roughly the same diameter tube.²²

Due to the stringent mass, volume, and power requirements on micropropulsion systems, the required preheat temperature and overall length of the tube to achieve peak performance is important. However, in order to assess these requirements, and in turn design an experimental thruster, basic properties of the propellant decomposition and burning behavior must be determined. This paper presents results on the experimental determination and assessment of the decomposition characteristics of the [Emim][EtSO₄]-HAN propellant on various catalytic surfaces through the use of a batch reactor. These measurements, taken together, can be used directly or compared to existing models of HAN propellant decomposition to aid the design of a catalytic microtube thruster. Section II will describe the setup of the experiment, Section III will present the results of the experiments, Section IV will discuss the results including relevant development or selection of decomposition model parameters, and Section V presents the conclusions of this study.

II. Experimental Setup

The batch reactor used in this study is similar in function to that used in the previous studies with the same propellant or other HAN-based propellants.^{9,15} The previous study on catalytic decomposition with the [Emim][EtSO₄] blend used a syringe to inject a droplet of the propellant onto pre-heated catalyst particles. Decomposition rate was determined by measuring the pressure change inside the reactor.⁹ This was done with application to a conventional monopropellant thruster in mind. In a chemical microtube, the monopropellant decomposition is initiated through heat and catalytic activity from the chamber walls instead of from many small catalyst particles packed into the chamber as in a conventional thruster. The batch reactor in this study therefore uses

heated metallic surfaces to generate decomposition of the monopropellant in order to best provide data for use in the design of a monopropellant microtube.

The reactor consists of a large (~1L) chamber with feedthroughs to accommodate heating of the catalyst surface and measurement of the surface temperature. Additionally, a gas feedthrough is used to evacuate the air in the chamber via mechanical vacuum pump, as well as to backfill with argon gas back to 15 psia pressure. The experimental setup in the lab is shown in Fig. 1. The propellant itself is held in place on top of the catalytic surface via the sample holder geometry shown in Fig. 2. The sample holder is a quartz tube with an inner diameter of 5.33 mm. The catalytic surface material is sandwiched between two sheets of Teflon material and the top sheet has a cutout of same diameter to the outside diameter of the sample holder cylinder. Additionally, a single strip of Teflon tape is wrapped around the base of the cylinder for experiments. This, combined with the high viscosity of the propellant, was found to provide an adequate seal to keep propellant from leaking out of the containment region provided by the cylinder. The catalytic material is heated by applying a voltage directly across the metallic material. For each experimental run, 50 μL of propellant is injected into the sample holder. The batch reactor is then closed off, evacuated, and back filled with argon. Finally, power is provided to the catalyst material until propellant decomposition is initiated. A thin wire type-K thermocouple measures the temperature of the catalyst surface throughout the duration of the experiment.



Figure 1. Photograph of the Batch Reactor Experiment in the Lab Showing Atmosphere Control Panel (left), Sample Holder (bottom), Pressure Measurement (right), and Temperature Measurement (top).

As mentioned, the propellant used in this study is a blend of hydroxylammonium nitrate (HAN) and 1-ethyl-3-methylimidazolium ethyl sulfate ([Emim][EtSO₄]) consisting of 59% oxidizer and 41% fuel by mass. The synthesis procedure is described in detail in the previous studies.^{9,13} Three catalyst materials are selected for this investigation: titanium, platinum, and rhenium. Rhenium was found from the previous study to be a good candidate catalyst material.⁹ Platinum was the material selected for the previous microtube thruster experiments¹⁰⁻¹² and is also a candidate for HAN propellant

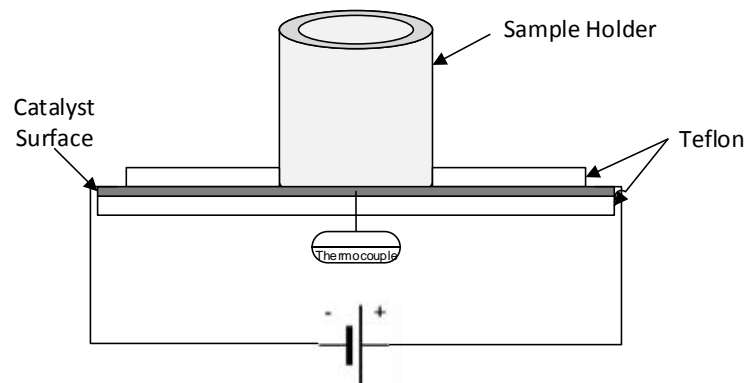


Figure 2. Illustration of the Sample Holder Geometry.

catalyst applications.¹⁵ Titanium is selected for this study to provide a measure of thermal decomposition absent catalytic activity since it is known to be compatible with HAN propellants for long term storage.^{19,23} The properties relevant to this study for each material are given in Table 1. For the experiment, a 25 mm x 8 mm strip of 0.025 mm thick material is used for platinum and rhenium. For titanium the dimensions are the same except for the thickness, which is 0.05 mm.

Table 1. Thermal and Electrical Properties of Catalyst Materials Used in This Study.

	ρ [Ω -m] x 10^{-7}	κ [W/m-K]	T_m [K]
Platinum	1.04	71.6	1968
Rhenium	1.85	71.0	3382
Titanium	4.27	20.8	1868

III. Results

Results from the batch reactor experiment described in the previous section are presented here. All decomposition experiments are conducted in a 15 psia argon internal atmosphere and with 50 μ L of propellant. For comparison, an 80% HAN/water blend and pure [Emim][EtSO₄] are also tested for decomposition with the same conditions used for the HAN/[Emim][EtSO₄] monopropellant blend. Results are displayed in terms of heat flux, which is calculated using the input current, material electrical resistivity and catalyst surface geometry. Due to differences in the material properties, exact heat flux could not be precisely replicated for all materials; however, relevant points will be addressed in the discussion section.

Sample results for the decomposition of the HAN/[Emim][EtSO₄] propellant on the catalyst surfaces are shown in Fig. 3. The figure shows the temperature indicated by the thermocouple as a function of time after power is applied through the catalyst surface. The results shown in the figure are for calculated input heat flux of 7.2, 7.9, and 13 mW/mm² for platinum, rhenium, and titanium, respectively. For all surface materials, the temperature increase is roughly linear initially, followed by a transition to another roughly linear region of higher slope, indicating exothermic decomposition of the monopropellant. The temperature at which decomposition of the propellant occurs, which for purposes of this study is taken as the start of the transition from the initial linear temperature slope, is lowest for platinum surface material at 85 °C, followed by rhenium at 125 °C and titanium at 165 °C. Since the rate of temperature increase during decomposition is driven by the exothermic reaction of the monopropellant also of note is that the rate of temperature increase is highest for platinum, which shows a sharp increase in temperature just after decomposition onset. Both rhenium and titanium show a longer transition region and peak at the end of the decomposition event.

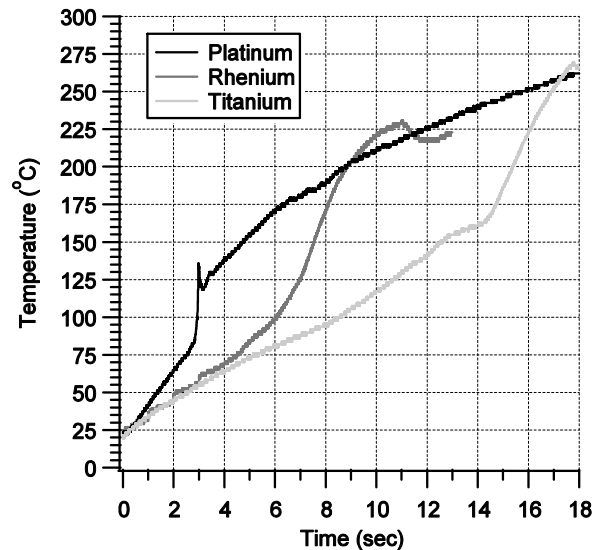


Figure 3. HAN/[Emim][EtSO₄] Monopropellant Decomposition on Platinum, Rhenium, and Titanium Surfaces.

The decomposition of the HAN/[Emim][EtSO₄] propellant is investigate further by conducting the experiment at various power input levels. Table 2 shows the results for each material at varied heat flux, which is again calculated from the input current and material properties. Results are shown in terms of temperature slope for the region before decomposition onset, during decomposition, and for the same input power with no propellant present. Additionally, for the case with no propellant present, the test is conducted at vacuum ($\sim 10^{-3}$ torr) instead of 15 psia argon. Temperature slope before decomposition and for the blank cases is taken as the line between points at $t = 0$ and $t = 2$ seconds. Temperature slope during decomposition is calculated by taking the line between two points as determined

by visual inspection of the temperature vs. time results similar to Fig. 3. Cases that did not result in decomposition during the test window of 18 seconds are given a dash-mark in the table. From the results shown in Fig. 3, platinum has the highest rate of temperature change during decomposition at 338-372 °C/sec. Tests on rhenium show higher rate of temperature change compared to titanium during the decomposition event, 51 °C/sec vs. 41.5 °C/sec respectively. Additionally, at similar heat flux, the platinum cases have a higher temperature slope before decomposition compared to both rhenium and titanium. For example, the temperature slope for heat flux of 3.2 mW/mm² is 7.5 °C/sec for platinum and 6.0 °C/sec for rhenium; and, the temperature slope is 10 °C/sec for platinum at 5 mW/mm² heat flux and 6.7 °C/sec at 5.4 mW/mm² for titanium. This trend is true for all cases tested. Tests on rhenium also show a slightly higher rate of temperature change prior to decomposition onset compared to titanium, for example 9.3 °C/sec at 4.3 mW/mm² on rhenium versus 8.5 °C/sec at 7 mW/mm² on titanium.

More information about the propellant decomposition process may be obtained by observing the decomposition of the constituent fuel and oxidizer. As mentioned, an 80% HAN by mass HAN/water solution and pure [Emim][EtSO₄] are tested for decomposition. Results on platinum at heat flux of 7.2 mW/mm² are shown in Fig. 4. From the figure, the decomposition onset of HAN/Water is virtually the same as that of the HAN/[Emim][EtSO₄] monopropellant blend. The temperature rate of change is the same value of 21.5 °C/sec, the onset temperature is 85 °C, and the temperature slope during decomposition is slightly lower for HAN/Water at 283 °C/sec. The behavior of temperature data after the decomposition event for HAN/Water is noticeably erratic; this will be discussed in the next section. Pure [Emim][EtSO₄] does show an exothermic decomposition peak, which has previously been observed qualitatively during spot plate tests.⁹ This occurs at roughly 140 °C on platinum, well above the decomposition onset of 85 °C for HAN/Water and HAN/[Emim][EtSO₄] blend.

IV. Discussion

Results from the preceding section are discussed, with particular attention paid to developing insights for the development of a

Table 2. Rate of Temperature Change Before and During Decomposition Events for Each Catalyst Surface at Various Input Power.

\dot{Q}'' (mW/mm ²)	\dot{T}_E (°C/s)	\dot{T}_S (°C/s)	\dot{T}_{blank} (°C/s)
<i>Platinum</i>			
3.2	7.5	-	10.0
4.4	9.5	354	17.7
5.0	10.0	363	27.0
6.0	15.0	338	31.7
7.2	21.5	372	37.5
<i>Rhenium</i>			
1.4	3.3	-	6.0
3.2	6.0	-	11.0
4.3	9.3	-	18.5
5.7	11.7	52	34.7
7.9	13.5	50	44.0
<i>Titanium</i>			
5.4	6.7	-	23.3
7.0	8.5	-	35
8.8	9.7	40	47.7
10.9	10.0	41	52.5
13.0	11.0	43	60.3

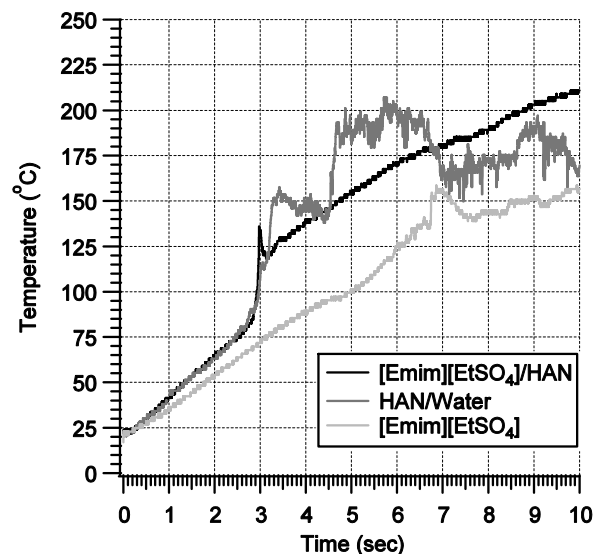


Figure 4. Decomposition of HAN/[Emim][EtSO₄] Monopropellant and Constituent Fuel and Oxidizer on Platinum.

microtube thruster. However, there is no reason why the results could not also be used, at minimum qualitatively, for catalyst development, particularly monolith catalysts. The results and trends seen in the previous section will first be discussed, followed by elucidation of these results into Arrhenius type reaction rate data.

A. Discussion of Experimental Results

The most significant result of the experiment is the fact that the lowest onset temperature and fastest decomposition rate of the monopropellant is obtained through the use of platinum material. Given that both platinum and rhenium show both lower onset temperature and faster decomposition rate than titanium, it is apparent that they do act as a catalyst for the monopropellant decomposition. The fact that the rate of temperature increase prior to the onset temperature is also greater for platinum and rhenium compared to titanium is likely indicative that the monopropellant is undergoing an exothermic adsorption process onto the metallic surface.

Further quantitative assessment of catalytic capability of platinum and rhenium requires the assumption that titanium does not act as a catalyst material for the HAN/[Emim][EtSO₄] monopropellant decomposition. The onset temperature for decomposition on titanium material was found in this study to be 165 °C. This agrees with the literature for the exothermic decomposition temperature for other HAN-based propellants, as well as HAN itself by thermal decomposition initiation means alone.^{15,24} Typically, for HAN-based propellants the initial step in the reaction is assumed to be the initial HAN decomposition step regardless of the fuel choice.^{18,25,26} This is mainly due to the fact that the fuel typically is not decomposed thermally, but through reaction with HAN decomposition intermediate species.²⁶ Results show that [Emim][EtSO₄] decomposes at much higher onset temperature than HAN for a particular catalyst, although it does appear to be catalyzed by platinum, as evidenced by the exothermic peak at 140 °C for pure [Emim][EtSO₄] but no such peak at at least 165 °C on titanium. Additionally, the HAN-water onset temperature is exactly the same as the HAN/[Emim][EtSO₄] propellant as seen in Fig. 4. It can therefore be reasonably concluded that titanium does not act as a catalyst for this monopropellant and that the fuel does not decompose thermally prior to the first step in HAN decomposition.

B. Elucidation of Arrhenius-Type Reaction Rate Data

Decomposition of HAN-based propellants, even assuming the fuel does not participate in the decomposition initiation, is comprised of many reaction steps.^{18,26} Without knowledge of the intermediate species, or post-reaction species it is not possible to determine a multi-step reaction mechanism from the data garnered in this experiment alone. However, in order to aid preliminary thruster design predictions it is useful to develop Arrhenius-type reaction rate equations for the decomposition of this monopropellant on various catalyst surfaces. Using the temperature vs. time data from this study it is possible to determine the activation energy and frequency factor for use in Eq. (1),

$$k' = Ae^{\frac{E}{k_B T}} \quad (1)$$

The energy balance for the system described in the experimental setup is Eq. (2),

$$\frac{dT}{dt} = \frac{\dot{Q} + (-\Delta H_{RX})(-r_A V)}{\sum N_i C_{p,i}} \quad (2)$$

where the contribution to temperature change is heat transfer from the electrical heating and self-heating from the exothermic decomposition of the monopropellant, Eqs. (3) and (4), respectively,

$$\dot{T}_E = \frac{\dot{Q}_E}{\sum N_i C_{p,i}} \quad (3)$$

$$\dot{T}_S = \frac{(-\Delta H_{RX})(-r_A V)}{\sum N_i C_{p,i}} \quad (4)$$

It is clear from the results that prior to the onset temperature the electrical heating rate is much greater than the self-heating rate and this region is therefore described fairly accurately by Eq. (3) except perhaps for the cases where

catalytic activity is observed. After the onset temperature is achieved the self-heating rate described by Eq. (4) clearly dominates the electrical heating rate. This data can therefore be used to determine the targeted reaction rate parameters. Substituting the Arrhenius rate equation into Eq. (4) and taking the natural logarithm of both sides gives Eq. (5),

$$\ln \dot{T}_s = \ln \left(\frac{(-\Delta H_{Rx})V}{\sum N_i C_{p,i}} \right) + \ln A + \ln C_A - \frac{E}{k_B T} \quad (5)$$

Since all parameters are constant aside from the temperature and self-heating rate, the activation energy is then the slope of the line of a plot of $\ln \dot{T}_s$ and $1/T$. The activity coefficient can then be solved for by substituting the result back into Eq. (5).

The results of these calculations are shown in Table 3. For the calculation of activity coefficient, the propellant specific heat was determined from Eq. (3) from the titanium data only since adsorption does

not occur and the only heating during the initial phase is due to electrical heating. The value of specific heat for this monopropellant is calculated to be 95.7 ± 8.6 J/mol-K. Results show what is expected from the assumed catalytic activity described previously, namely that the platinum surface yields the lowest activation energy, followed by rhenium.

Table 3. Arrhenius Rate Equation Parameters Calculated from Experimental Data.

Material	E/k _B (K)	A (mL/mol-sec)
Platinum	10771 ± 503	(3.87 ± 0.23) × 10 ¹²
Rhenium	16170 ± 107	(1.02 ± 0.26) × 10 ¹⁷
Titanium	30111 ± 797	(1.31 ± 0.26) × 10 ¹⁹

V. Conclusion

A monopropellant blend of hydroxylammonium nitrate and [Emim][EtSO₄] was tested on platinum, rhenium, and titanium surfaces in order to garner data for use in microtube thruster or monolith catalyst bed design. When heated on a titanium surface, the monopropellant decomposes at 165 °C, which agrees with the known decomposition temperature for hydroxylammonium nitrate. Furthermore, the fuel decomposes exothermically at a much higher temperature, which suggests that the reaction mechanism for this monopropellant blend is initiated by HAN decomposition and intermediate species react to decompose the fuel, which agrees with insights from other studies utilizing different fuels.

It was found that platinum and rhenium exhibit catalytic activity for the HAN/[Emim][EtSO₄] propellant blend, with platinum initiating decomposition at 85 °C and rhenium at 125 °C. Use of these materials will therefore lessen power requirements to start monopropellant rocket engines using this propellant. Platinum initiates the highest rate of reaction, but the material melts at near the flame temperature of the propellant⁸. The flame temperature, however, could be reduced by increasing the fuel mass fraction in the monopropellant bend. Since the decomposition is likely initiated by HAN decomposition and the fuel is then attacked by the reaction intermediates, increasing the fuel ratio of the monopropellant blend could allow use of platinum as a catalyst to start the thruster and thus reduce overall propulsion system power requirements.

References

- ¹Kluever, C. A., "Spacecraft Optimization with Combined Chemical-Electric Propulsion," *Journal of Spacecraft and Rockets*, Vol. 32, No. 2, 1994, pp. 378-380.
- ²Kluever, C. A., "Optimal Geostationary Orbit Transfers Using Onboard Chemical-Electric Propulsion," *Journal of Spacecraft and Rockets*, Vol. 49, No. 6, 2012, pp. 1174-1182.
- ³Oh, D. Y., Randolph, T., Kimbrel, S., and Martinez-Sanchez, M., "End-to-End Optimization of Chemical-Electric Orbit Raising Missions," *Journal of Spacecraft and Rockets*, Vol. 41, No. 5, 2004, pp. 831-839.
- ⁴Oleson, S. R., Myers, R. M., Kluever, C. A., Riehl, J. P., Curran, F. M., "Advanced Propulsion for Geostationary Orbit Insertion and North-South Station Keeping," *Journal of Spacecraft and Rockets*, Vol. 34, No. 1, 1997, pp. 22-28.
- ⁵Donius, B. R. and Rovey, J. L., "Ionic Liquid Dual-Mode Spacecraft Propulsion Assessment," *Journal of Spacecraft and Rockets*, Vol. 48, No. 1, 2011, pp. 110-123.
- ⁶Haas, J. M., and Holmes, M. R., "Multi-Mode Propulsion System for the Expansion of Small Satellite Capabilities," Air Force Research Laboratory, Rept. NATO MP-AVT-171-05, 2010.

⁷Berg, S. P., and Rovey, J. L., "Assessment of Multi-Mode Spacecraft Micropropulsion Systems," *Journal of Spacecraft and Rockets*, Vol. No. 2016, pp. in review; also AIAA Paper 2014-3758, July 2014.

⁸Berg, S. P., and Rovey, J. L., "Assessment of Imidazole-Based Energetic Ionic Liquids as Dual-Mode Spacecraft Propellants," *Journal of Propulsion and Power*, Vol. 29, No. 2, 2013, pp. 339-351.

⁹Berg, S. P., and Rovey, J. L., "Decomposition of Monopropellant Blends of Hydroxylammonium Nitrate and Imidazole-Based Ionic Liquid Fuels," *Journal of Propulsion and Power*, Vol. 29, No. 1, 2013, pp. 125-135.

¹⁰Mento, C. A., Sung, C.-J., Ibarreta, A. F., Schneider, S. J., "Catalyzed Ignition of Using Methane/Hydrogen Fuel in a Microtube for Microthruster Applications," *Journal of Propulsion and Power*, Vol. 25, No. 6, 2009, pp. 1203-1210.

¹¹Boyarko, G. A., Sung, C.-J., Schneider, S. J., "Catalyzed Combustion of Hydrogen-Oxygen in Platinum Tubes for Micropropulsion Applications," *Proceedings of the Combustion Institute*, Vol. 30, No. 2, 2005, pp. 2481-2488.

¹²Volchko, S. J., Sung, C.-J., Huang, Y., Schneider, S. J., "Catalytic Combustion of Rich Methane/Oxygen Mixtures for Micropropulsion Applications," *Journal of Propulsion and Power*, Vol. 22, No. 3, 2006, pp. 684-693.

¹³Berg, S. P., Rovey, J. L., Prince, B. P., Miller, S. W., and Bemish, R.J., "Electrospray of an Energetic Ionic Liquid for Multi-Mode Micropropulsion Applications," *Journal of Propulsion and Power*, Vol. No. 2016, pp. in review; also AIAA Paper 2015-4011, July 2014.

¹⁴Sutton, G. P., and Biblarz, O., *Rocket Propulsion Elements*, 7th ed., Wiley, New York, 2001.

¹⁵Elroidi, R., Rossignol, S., Kappenstein, C., Duprez, D., Pillet, N., "Design and Use of a Batch Reactor for Catalytic Decomposition of Propellants," *Journal of Propulsion and Power*, Vol. 19, No. 2, 2003, pp. 213-219.

¹⁶Slettenhaar, B., Zevenbergen, J. F., Pasman, H. J., Maree, A. G. M., and Morel, J. L. P. A., "Study on Catalytic Ignition of HNF Based Non Toxic Monopropellants," *39th AIAA/ASME/SAE/ASEE Joint Propulsion Conference & Exhibit*, AIAA Paper 2003-4920, 2003.

¹⁷Anflo, K., Mollerberg, R., "Flight Demonstration of New Thruster and Green Propellant Technology on the PRISMA Satellite," *Acta Astronautica*, Vol. 65, No. 9-10, 2009, pp. 1238-1249.

¹⁸Lee, H.-S., Litzinger, T. A., "Chemical Kinetic Study of HAN Decomposition," *Combustion and Flame*, Vol. 135, No. 1-2, 2003, pp. 151-169.

¹⁹McLean, C. H., Deininger, W. D., Joniatis, J., Aggarwal, P. K., Spores, R. A., Deans, M., Yim, J. T., Bury, K., Martinez, J., Cardiff, E. H., Bacha, C. E., "Green Propellant Infusion Mission Program Development and Technology Maturation," *50th AIAA/ASME/SAE/ASEE Joint Propulsion Conference*, AIAA Paper 2014-3481, 2014.

²⁰Chiu, Y., Dressler, A., "Ionic Liquids for Space Propulsion", *Ionic Liquids IV: Not Just Solvents Anymore*, Vol. 975, American Chemical Society, Washington, D. C., 2007, Ch. 10.

²¹Gamero-Castano, M., "Characterization of a Six-Emitter Colloid Thruster Using a Torsional Balance," *Journal of Propulsion and Power*, Vol. 20, No. 4, 2004, pp. 736-741.

²²Alexander, M. S., Stark, J., Smith, K. L., Stevens, B., Kent, B., "Electrospray Performance of Microfabricated Colloid Thruster Arrays," *Journal of Propulsion and Power*, Vol. 22, No. 3, 2006, pp. 620-627.

²³Schmidt, E. W., "Hydroxylammonium Nitrate Compatibility Tests with Various Materials-A Liquid Propellant Study," U.S. Army Ballistic Research Laboratory, Rept. BRL-CR-636, 1990.

²⁴Alfano, A. J., Mills, J. D., Vaghjiani, G. L., "Resonant Laser Ignition Study of HAN-HEHN Propellant Mixture," *Combustion Science and Technology*, Vol. 181, No. 6, 2009, pp. 902-913.

²⁵Vosen, S. R., "Hydroxylammonium nitrate-based liquid propellant combustion-interpretation of strand burner data and the laminar burning velocity," *Combustion and Flame*, Vol. 82, No. 3-4, 1990, pp. 376-388.

²⁶Chang, Y.-P., "Combustion Behavior of HAN-Based Liquid Propellants," Mechanical Engineering, Pennsylvania State University, 2002.